ISBN: 978-3-95450-222-6 ISSN: 2673-5350 doi:10.18429/JACoW-IBIC2020-TUPP28

SIMULATION OF CHERENKOV DIFFRACTION RADIATION FOR VARIOUS RADIATOR DESIGNS

K. Lasocha*[1], T. Lefevre, N. Mounet, A. Schloegelhofer[2], CERN, Geneva, Switzerland
D. M. Harryman, JAI, Royal Holloway, University of London, Egham, Surrey, UK
[1]also at Institute of Physics, Jagiellonian University, Krakow, Poland
[2]also at TU Wien, Vienna, Austria

Abstract

Studies performed during the last few years at different facilities have indicated that the emission of Cherenkov Diffraction Radiation (ChDR) can be exploited for a range of non-invasive diagnostics. The question remains of how to choose an optimal dielectric material and which radiator shapes give the most promising results. This contribution presents a semi-analytical framework for calculating the electromagnetic field of a charged particle beam, taking into consideration its interaction with surrounding structures. It allows us to directly compute ChDR at arbitrary probe positions inside the radiator. Several configurations will be discussed and presented, including flat and cylindrical radiators of various dimensions and electrical properties, as well as multilayer structures obtained by adding coatings of metallic nanolayers.

INTRODUCTION

A decade after the discovery of Cherenkov radiation [1], Ginzburg and Frank [2] studied the radiation emitted by a particle moving along the axis of an infinitely long evacuated tunnel surrounded by a dielectric medium. During the following decades Linhart [3] and Ulrich [4] described a similar phenomenon associated with a particle moving parallel to the surface of a dielectric half space. These two are the initial examples of Cherenkov Diffraction Radiation (ChDR), which describes the emitted radiation of a charged particle passing in the close vicinity of a dielectric medium and having a velocity greater than the phase velocity of light in that medium.

Recently, the possibilities which ChDR brings to non-invasive beam diagnostics have been extensively investigated, with the first observation of incoherent radiation, using GeV electrons and positrons at Cornell [5, 6]. What followed were designs of beam position monitors [7] as well as bunch length monitors [8] based on the coherent radiation from short bunches. In parallel more refined radiation models have been developed [9, 10]. In addition, several accelerator facilities across the world have confirmed the feasibility of observing ChDR [11–13].

All this interest motivates the need of developing a tool for quantitative description of ChDR for real case scenarios. Most analytic models serve well only in a limited spectrum of cases, due to the simplicity of the considered radiators. On the other hand, more flexible numerical simulations are very time consuming, especially if the radiator components differ significantly in size. The aim of this contribution is to present a semi-analytical approach, which is based on numerical calculations of the beam field propagating across surrounding materials, according to constraints set by the Maxwell equations. The presented procedure describes radiators infinite in the direction of beam propagation, but gives the possibility of studying complex multilayer structures orthogonal to the direction of beam propagation. The proposed method should be treated as a natural extension of a framework for beam impedance calculations, developed at CERN [14].

CYLINDRICAL GEOMETRY

We shall start by considering the geometry presented in Fig. 1 which is described using cylindrical coordinates r, θ and s. A charged particle travels with the velocity $v = \beta c$ along the s axis in the centre of an axisymmetric structure, consisting of an arbitrary number of layers. Each layer has its own permittivity ϵ_i and permeability μ_i, which may be frequency dependent. The central layer is constrained to be vacuum, but the subsequent layers may be any material, with the outermost layer extending to infinity.

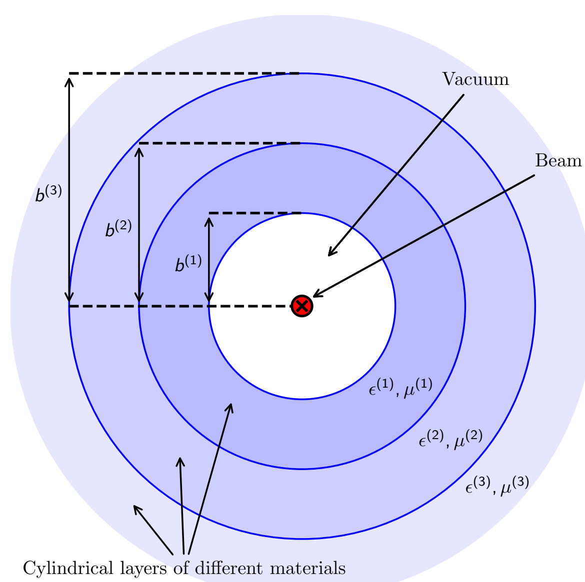

Figure 1: Cylindrical geometry with concentric layers of different materials. The beam travels along the axis perpendicular to the page.

* kacper.lasocha@cern.ch

Content from this work may be used under the terms of the CC BY 3.0 licence (© 2020). Any distribution of this work must maintain attribution to the author(s), title of the work, publisher, and DOI

ISBN: 978-3-95450-222-6 ISSN: 2673-5350 doi:10.18429/JACoW-IBIC2020-TUPP28

Content from this work may be used under the terms of the CC BY 3.0 licence (© 2020). Any distribution of this work must maintain attribution to the author(s), title of the work, publisher, and DOI

The longitudinal component of the electric and magnetic field ($E_s^{(p)}$ and $H_s^{(p)}$) in a probe point at a distance r from the axis, located in layer p, have the following explicit form in frequency domain:

$$E_s^{(p)} = e^{-jks}\left[C_{Ie}^{(p)} I_0(\nu^{(p)}r) + C_{Ke}^{(p)} K_0(\nu^{(p)}r)\right], \quad (1)$$

where I_0 and K_0 are zero-order modified Bessel functions of first and second kind respectively, $k = \frac{\omega}{v}$ is a wave number and $\nu^{(p)} = |k|\sqrt{1-\beta^2\epsilon_p\mu_p}$ is a radial propagation constant. This follows from [14, Eq. (1.85)] by noting that for a centered beam all modes apart from $m = 0$ do not contribute to the field. The complex coefficients $C_{Ie}^{(p)}$ and $C_{Ke}^{(p)}$ depend on frequency, particle velocity and the considered structure. Their explicit calculation is thoroughly shown in [14, Ch. 1.4]. What should be emphasized, is that their computation involves only a small number of Bessel function evaluations and matrix multiplications, and is therefore very fast. The longitudinal component of the magnetic field can be expressed in a similar manner, but it turns out that $H_s^{(p)} = 0$.

Based on Maxwell's equations we can also derive the transverse component of both fields [14, Appx. E.1.1]. The only non-zero transverse components will be E_r and H_θ. In order to derive the time integrated radiated energy, we define

$$\vec{P}(\omega) = \Re\left[\vec{E}(\omega) \times \vec{H}^*(\omega)\right],$$

where $\vec{H}^*$ is the complex conjugate of the magnetic field $\vec{H}$ and $\Re\left[\cdot\right]$ denotes the real part of a vector. The energy radiated outside a given volume V that contains the beam, is given by

$$\Delta E = \frac{1}{2\pi}\int d\omega \oiint\limits_{\mathbf{A}=\partial V} \vec{P}(\omega)\cdot d\mathbf{A}, \quad (2)$$

as a consequence of the Poynting theorem.

FLAT GEOMETRY

The next geometry considered is a flat geometry described using Cartesian coordinates x, y and s. This consists of a series of infinitely long (in s direction) and wide (in x direction) plates, each having its own thickness, permittivity ϵ_i and permeability μ_i. A charged particle travels in the s direction inside the central layer, which again we constraint to be vacuum. It is also assumed that the top and bottom outermost layers are infinitely thick. An example of such a structure is presented in Fig. 2.

Let us pick a probe point $P = (x, y, s)$ placed in layer p. The longitudinal component of the electric and magnetic field are of the form [14, Eq. (1.180,1.181)]:

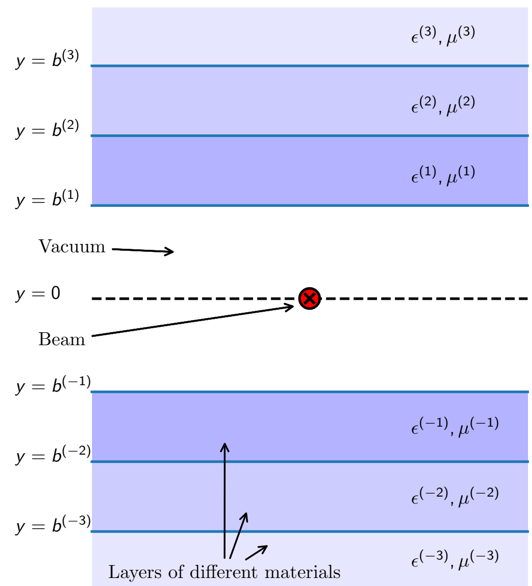

Figure 2: Flat geometry with parallel layers of different materials. The beam travels perpendicular to the page in the plane $y = 0$.

$$E_s^{(p)} = e^{-jks} \times \int_0^\infty dk_x \cos(k_x x)\left[C_{e+}^{(p)}(k_x)e^{k_y^{(p)}y} + C_{e-}^{(p)}(k_x)e^{k_y^{(p)}y}\right],$$

$$H_s^{(p)} = e^{-jks} \times \int_0^\infty dk_x \sin(k_x x)\left[C_{h+}^{(p)}(k_x)e^{k_y^{(p)}y} + C_{h-}^{(p)}(k_x)e^{k_y^{(p)}y}\right],$$

where $k_y^{(p)} = \sqrt{k_x^2 + \nu^{(p)2}}$ is the vertical wave number, with $\nu^{(p)}$ defined as in the previous section. Coefficients $C_{e\pm}, C_{h\pm}$ again depend on k_x, frequency and the properties of all the layers, but this time their calculation requires a time-consuming matrix inversion (all the related details can be found in [14, Ch. 1.5]). On top of that, due to the complicated form of the integrand, the integration needs to be performed numerically. This all results in much slower field calculations than in the case of cylindrical geometry. The transverse components of the electromagnetic field can be derived from the longitudinal ones in the classical way, see [14, Appx. E.2.1]. Having all the components we can calculate the radiated energy in the same way as in the previous section.

CHERENKOV DIFFRACTION RADIATION

The geometries discussed in the two previous sections are suitable to study the properties of ChDR. To do this we choose the outermost layer to be a dielectric and place the

ISBN: 978-3-95450-222-6 ISSN: 2673-5350 doi:10.18429/JACoW-IBIC2020-TUPP28

probe point at a given depth inside this layer. The dielectric layer is set to be infinitely thick in order to avoid reflections from its outermost surface. By creating a grid of probe points, we are able to estimate either a total radiated energy, using Eq. (2), or the spatial distribution of the radiation.

Figure 3 shows the spectral distribution of the energy emitted by a point particle with a charge equivalent to 1 C, which travels a distance of 1 m along the axis of a vacuum cylinder of radius r. The cylinder is surrounded by an infinite dielectric with a refractive index of $n = 2$. The velocity of the point particle corresponds to $\gamma = 10$. As a reference, we plot the distribution for Cherenkov radiation emitted by a particle passing directly through the medium, obtained from the classical Frank-Tamm formula [15]:

$$\frac{dE}{dx} = \frac{q^2}{4\pi} \int_{v > \frac{c}{n(\omega)}} \mu(\omega)\omega\left(1 - \frac{c^2}{v^2 n^2(\omega)}\right) d\omega.$$

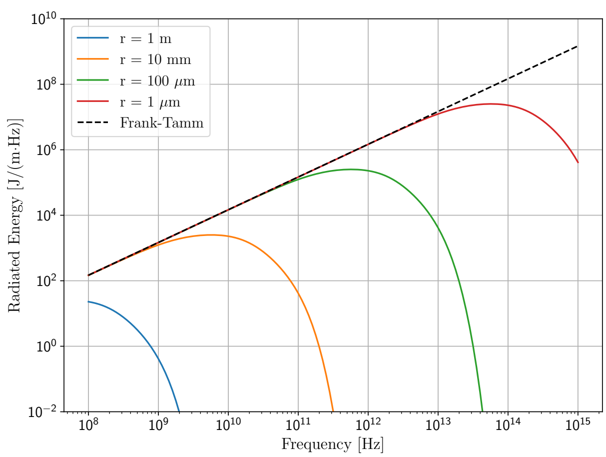

Figure 3: Comparison between Frank-Tamm formula (Cherenkov radiation) and Eq. (2) with decreasing chamber radii (ChDR).

As can be seen in Fig. 3 the calculated distributions follow the Frank-Tamm formula for $\omega \ll \frac{\gamma c}{r}$. On the other hand, for $\omega \gg \frac{\gamma c}{r}$ the amount of radiated energy drops abruptly. This is in agreement with the notion of effective radius, that is the distance over which the particle's field interacts with the surrounding medium, determined in [10] to be $r_{\text{eff}} = \frac{\gamma c}{\omega}$. The presented model based on beam field calculations yields not just qualitative, but quantitative results, which coincide with the well-established Frank-Tamm formula.

SPATIAL DISTRIBUTION OF CHDR

A dense grid of probe points, in which we calculate EM field components, allows us to estimate the spatial distribution of the radiation and monitor which parts of the radiator interact with the beam. To illustrate such an analysis we take the example of one of the experiments reported in [5]. A flat radiator made of fused silica ($n = 1.45$) mounted above of the beam is considered, with a parallel bunched beam of velocity corresponding to $\gamma \approx 10373$. We consider four different vertical impact parameters, that is to say the distance between the axis of the beam and radiator surface: 0.9 mm, 1.08 mm, 1.32 mm and 1.38 mm. A series of probes is placed 2 mm inside the dielectric at different x offset with respect to the beam. For every probe we calculate the vector $\vec{P}(\omega)$ in order to estimate the radiation intensity. The y component of this vector is convoluted with the transverse bunch profile, which is assumed to be a 2-D Gaussian with $\sigma_x = 1.7$ mm, $\sigma_y = 170\,\mu$m. These values correspond to the beam parameters of [5]. Note that in order to convolute the results from this particle distribution, simulations are run with impact parameters different from the four mentioned above. The results are plotted in Fig. 4 for $\omega = 600$ THz and can be compared with [5, Fig. 4].

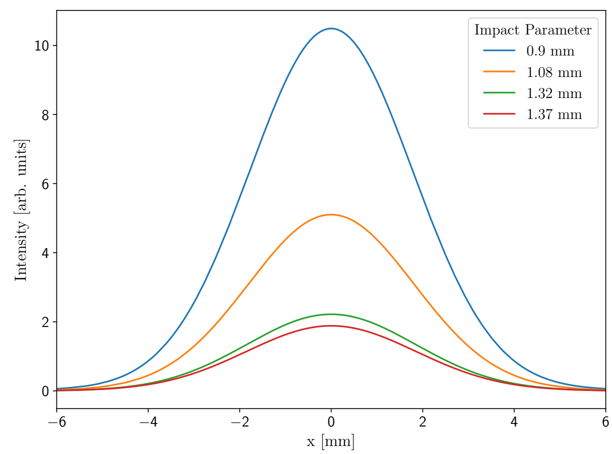

Figure 4: Horizontal profile of ChDR (600 THz) at a depth of 2 mm inside the flat dielectric.

It is interesting to see how the width of the discussed distribution increases with the impact parameter, as this can be compared with the experimental observations [6]. The corresponding values are given in terms of Full Width at Half Maximum (FWHM) in Table 1.

Table 1: Full Width at Half Maximum of ChDR (600 THz) Horizontal Profile at a Depth of 2 mm Inside the Flat Dielectric

Impact Par. [mm]	FWHM [mm]
0.9	4.19
1.08	4.25
1.32	4.33
1.37	4.35

METALLIC NANOLAYERS

The presence of a thin metallic layer between the beam and the dielectric may lead to the excitation of Surface Plasmon Polaritons (SPP) on the metal-vacuum and metal-dielectric intersection. As a consequence, one observes the creation

Content from this work may be used under the terms of the CC BY 3.0 licence (© 2020). Any distribution of this work must maintain attribution to the author(s), title of the work, publisher, and DOI

ISBN: 978-3-95450-222-6 ISSN: 2673-5350 doi:10.18429/JACoW-IBIC2020-TUPP28

Content from this work may be used under the terms of the CC BY 3.0 licence (© 2020). Any distribution of this work must maintain attribution to the author(s), title of the work, publisher, and DOI

of monochromatic Cherenkov radiation with significantly enhanced intensity for particular frequencies [16].

We shall demonstrate this effect with the following setup: a point particle with a charge of 11 fC travels with a velocity corresponding to $\gamma \approx 118.42$ inside a thin silver cylinder surrounded by an infinite layer of a dielectric with a refractive index of $n = 1.45$. The cylinder radius is 200 nm and the silver layer is 80 nm thick. The radius and beam properties correspond to typical beam parameters and dimensions of a Dielectric Laser Accelerator (DLA), reported in [17]. Considering a point charge instead of a distributed electron bunch is a simplification which will require further correction depending on the bunch profile.

As Eq. (1) requires knowledge of the permittivity of silver, we adopt the Drude model [18]

$$\epsilon = \epsilon_\infty - \frac{\omega_p^2}{\omega^2 - j\gamma\omega},$$

where for silver $\epsilon_\infty = 5.3$ (high-frequency permittivity limit), $\omega_p = 1.39 \times 10^{16}$ rad/s (plasma frequency) and $\gamma = 3.2 \times 10^{13}$ Hz (damping constant), as given in [16].

In Fig. 5 we present the spectral distribution of the energy radiated in the case of just the bare dielectric, calculated as described in the previous sections, and in the case of an added 80 nm thick silver coating. As we see, the presence of the metallic layer has transformed a broad ChDR spectrum into a monochromatic visible radiation of significantly higher intensity at that wavelength. The thickness of the metal layer was chosen in order to maximize this effect.

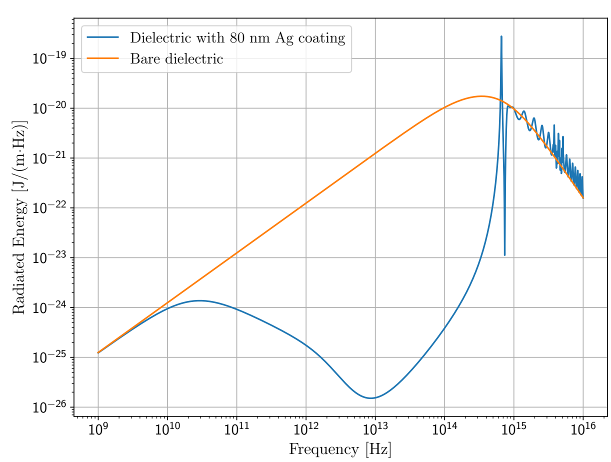

Figure 5: Surface Plasmon Polariton resonance at 660 THz in the geometry compatible with Dielectric Laser Accelerator described in [17].

CONCLUSION

The described theory has been implemented in the form of C++ code with a Python wrapper included. In addition, actions toward integrating it with Polarisation Currents Approach (PCA) [19] to form a single, independent simulation package are ongoing. In the course of this integration a comparison between PCA and the presented approach will be performed to validate the spectral properties of the radiation.

The approach presented in this contribution facilitates calculation of ChDR spectral distributions. In particular, it enables the effect of using multilayer radiators composed of various materials (metals, dielectrics, lossy media) to be studied. The parameters of these layers may be then tuned in order to either maximize the expected radiation output or reshape the spectral distribution. Contrary to previous models, this method provides the spatial, rather than angular, distributions of the radiation. This allows investigating how, and over which volume, the beam field interacts with the materials in different layers and generates radiation.

For applications in beam instrumentation, depending on the accelerator parameters and environment, coating the surface of the dielectric with metallic layers might be useful. It can for example prevent the building up of electron cloud on the dielectric in circular machines. Thin metallic layers, as discussed in this paper would also provide a way to produce a more monochromatic Cherenkov emission through the generation of surface plasmonic wave. In addition, within the model's capabilities is evaluating the expected photon flux, assessing beam position monitors sensitivity, or testing the impact of unsought oxidation of radiator elements.

ACKNOWLEDGEMENTS

The authors would like to express their gratitude for the stimulating discussions with D. Alves.

REFERENCES

[1] P. Čerenkov, "Visible radiation produced by electrons moving in a medium with velocities exceeding that of light", *Physical Review*, vol. 52, no. 4, p. 378, 1937.

[2] V. L. Ginzburg and I. M. Frank, *Doklady Akad. Nauk S.S.S.R.*, vol. 56, no. 699, 1947.

[3] J. G. Linhart, "Čerenkov Radiation of Electrons Moving Parallel to a Dielectric Boundary", *Journal of Applied Physics*, vol. 26, no. 5, pp. 527–533, 1955.

[4] R. Ulrich, "Zur Cerenkov-Strahlung von Elektronen dicht über einem Dielektrikum", *Zeitschrift fur Physik*, vol. 194, pp. 180–192, 1966.

[5] R. Kieffer *et al.*, "Direct Observation of Incoherent Cherenkov Diffraction Radiation in the Visible Range", *Phys. Rev. Lett.*, vol. 121, p. 054802, 2018. doi:10.1103/physrevlett.121.054802

[6] R. Kieffer *et al.*, "Generation of incoherent cherenkov diffraction radiation in synchrotrons", *Phys. Rev. Accel. Beams*, vol. 23, p. 042803, 2020. doi:10.1103/PhysRevAccelBeams.23.042803

[7] T. Lefevre *et al.*, "Cherenkov Diffraction Radiation as a tool for beam diagnostics", in *Proc. IBIC'19*, Malmö, Sweden, Sep. 2019, paper THAO01, pp. 660. doi:10.18429/JACoW-IBIC2019-THAO01

ISBN: 978-3-95450-222-6 ISSN: 2673-5350 doi:10.18429/JACoW-IBIC2020-TUPP28

[8] A. Curcio *et al.*, “Noninvasive bunch length measurements exploiting Cherenkov diffraction radiation”, *Phys. Rev. Accel. Beams*, vol. 23, p. 022802, 2020. doi:10.1103/PhysRevAccelBeams.23.022802

[9] M. Shevelev and A. Konkov, “Peculiarities of the generation of Vavilov-Cherenkov radiation induced by a charged particle moving past a dielectric target”, *J. Exp. Theor. Phys.*, vol. 118, pp. 501–511, 2014. doi:10.1134/S1063776114030182

[10] D. V. Karlovets and A. P. Potylitsyn, “Universal description for different types of polarization radiation”, 2009. arXiv:0908.2336

[11] D. M. Harryman *et al.*, “First Measurements of Cherenkov-Diffraction Radiation at Diamond Light Source”, in *Proc. IBIC'19*, Malmö, Sweden, Sep. 2019, paper WEPP037, pp. 624. 10.18429/JACoW-IBIC2019-WEPP037

[12] K. V. Fedorov, Y. M. Saveliev, A. N. Oleinik, P. Karataev, A. Potylitsyn, and T. H. Pacey, “Experimental Observation of Submillimeter Coherent Cherenkov Radiation at CLARA Facility”, in *Proc. IBIC'19*, Malmö, Sweden, Sep. 2019, paper TUCO02, pp. 261. doi:10.18429/JACoW-IBIC2019-TUCO02

[13] S. Ninomiya *et al.*, “Measurement of Cherenkov Diffraction Radiation from a Short Electron Bunches at t-ACTS”, in *Proc. IPAC'19*, Melbourne, Australia, May 2019, pp. 2536–2538. doi:10.18429/JACoW-IPAC2019-WEPGW031

[14] N. Mounet, “The LHC Transverse Coupled-Bunch Instability”, Ph.D. Thesis, École Polytechnique Fédérale de Lausanne, Lausanne, Switzerland, 2012.

[15] I. Frank and I. Tamm, “Coherent visible radiation of fast electrons passing through matter”, *Compt. Rend. Acad. Sci. URSS*, vol. 14, no. 3, pp. 109–114, 1937.

[16] S. Liu *et al.*, “Surface Polariton Cherenkov Light Radiation Source”, *Phys. Rev. Lett.*, vol. 109, p. 153902, 2012. doi:10.1103/PhysRevLett.109.153902

[17] E. Peralta *et al.*, “Demonstration of electron acceleration in a laser-driven dielectric microstructure”, *Nature*, vol. 503, p. 91, 2013. doi:10.1038/nature12664

[18] P. Drude, “Zur Elektronentheorie der Metalle; II. Teil. Galvanomagnetische und thermomagnetische Effecte”, *Annalen der Physik*, vol. 308, pp. 369–402, 1900.

[19] D. M. Harryman *et al.*, “Properties of Cherenkov Diffraction Radiation as Predicted by the Polarisation Currents Approach for Beam Instrumentation”, presented at the IBIC'20, Santos, Brazil, Sep. 2020, paper THPP05, this conference.

Content from this work may be used under the terms of the CC BY 3.0 licence (© 2020). Any distribution of this work must maintain attribution to the author(s), title of the work, publisher, and DOI